

Nonergodicity in binary alloys.

Leonid Son¹, Valery Sidorov², Pjotr Popel², Dmitry Shulgin¹

¹ Ural Federal University, 19 Mira st., 620002, Ekaterinburg, Russia

² Ural State Pedagogical University, 18 Cosmonavtov ave., 620219, Ekaterinburg, Russia

E-mail: ldson@yandex.ru

Abstract. For binary liquids with limited miscibility of the components, we provide the corrections to the equation of state which arise from the nonergodic diffusivity. It is shown that these corrections result in lowering of critical miscibility point. In some cases, it may result in a bifurcation of miscibility curve: the mixtures near 50% concentration which are homogeneous at the microscopic level, occur to be too stable to provide a quasi - eutectic triple point. These features provide a new look on the phase diagrams of some binary systems. In present work, we discuss Ga-Pb, Fe-Cu, and Cu-Zr alloys. Our investigation corresponds their complex behavior in liquid state to the shapes of their phase diagrams.

1. Introduction

Traditional approach to the statistics and dynamics of binary mixture consisting of atoms of A and B type is based on a coarsened lattice gas model. Namely, it is supposed that possible atomic positions correspond to the sites of spatial lattice. Possible configurations of the mixture are described in terms of filling numbers $n(r)$, where r is the coordinate of the site, and $n(r) = 1$ if the site is occupied by the atom of A type, and $n(r) = 0$ for the atom of B type. Then, one introduces the effective Hamiltonian for certain spatial configuration of variables $\{n(r)\}$:

$$H\{n\} = -\frac{1}{2} \sum_{r,r'} n(r)J(r-r')n(r') - \sum_r \mu(r)n(r), \quad (1)$$

Hamiltonian (1) serves to provide Gibbs statistics (but, in contrast with "real" Hamiltonian, does not determine the dynamics!). Then, the statistics and thermodynamics are described by partition Z and thermodynamic potential G :

$$Z = \sum_{\{n\}} \exp \left[-\frac{H\{n\}}{T} \right], \quad G = -T \ln Z \quad (2)$$

To calculate the partition, one uses the mean field (MF) approximation, which replaces full statistics with statistics of single site variable $n(r)$, embedded into surrounding "field" of neighboring sites. For these sites, one suggests mean value of filling number $\langle n(r) \rangle = x(r)$. For this single site, the partition includes only two terms

$$Z_{MF} = \sum_{n=0,1} \exp \left[n \frac{J}{T} x + n \frac{\mu}{T} \right] = 1 + \exp \left[\frac{J}{T} x + \frac{\mu}{T} \right], \quad (3)$$



where

$$J = \sum_{r'} J(r - r'). \quad (4)$$

Using (3), one easily calculates the mean value $\langle n(r) \rangle$. Obvious self consistency $x = \langle n(r) \rangle$ gives the well known mean - field equation on the mean concentration x :

$$\frac{T}{J}x = \frac{\exp(x + \nu)}{1 + \exp(x + \nu)}. \quad (5)$$

The dimensionless chemical potential ν serves as a Lagrange multiplier to fix out the concentration. This equation at $T > J/4$ has only one solution for all ν , but at $T \leq J/4$ in the vicinity of $x = 0.5$ it splits up in two solutions, and this split results in miscibility gap. Thus, the concentration - temperature phase diagram looks as a cupola dividing two - phase and single - phase domains. This is statistical base of regular solutions theory.

2. Nonergodic behavior of binary mixtures.

Hibbs statistics is based on the ergodic hypothesis, which implies that states with equal energies have equal probabilities. At the same time, binary system has obvious dynamical limitations, arising from the principle of local equilibrium: atom cannot disappear at one spatial point and appear at another at once, so starting from some certain configuration, system can not reach some configurations per observation time, in spite of the fact that those have big Hibbs probability. In [1, 2] we accounted these limitations. It was shown, that below $T = J/4$, equation (5) should be rewritten as

$$\frac{T}{J}x = \frac{e^\beta}{1 + e^\beta} + C \frac{e^\beta(1 - e^\beta)}{(1 + e^\beta)^3}, \quad \beta = x + \nu \quad (6)$$

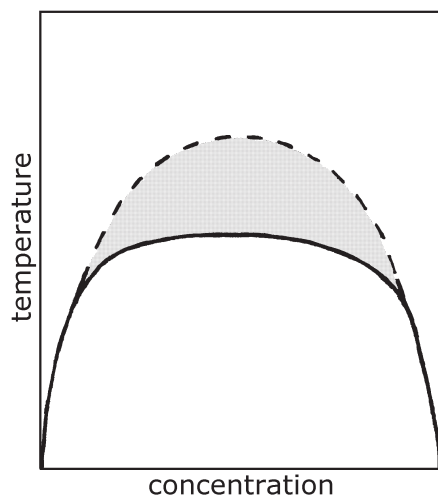


Figure 1. Phase diagram according to (5) is drawn by dashed line. Solid line corresponds to (6)

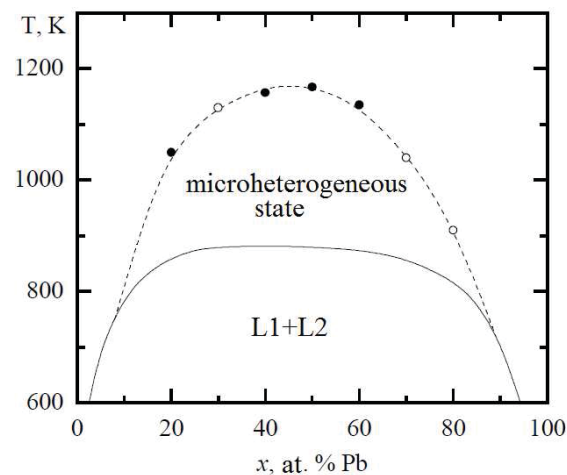


Figure 2. Miscibility cupola in Ga-Pb system and microheterogeneous area [3], obtained by ultrasonic technique. Dark and open circles correspond to the samples obtained by different smelting regimes

In [1, 2] equation (6) was obtained by strict accounting of dynamical limitations. It may be derived via mathematically not rigorous but simple considerations. Below $T = J/4$, the tendency to the phase separation occurs, and system becomes microheterogeneous: some local volumes

become enriched with component A, while others - with component B. This microheterogeneity may be described by random spatial fluctuations of chemical potential:

$$\nu(r) = \nu + \Delta\nu(r). \quad (7)$$

Thus, one gets a set of equations (5) in different spatial points with different $\nu(r)$. Suggesting smallness of $\Delta\nu$, one can expand (5) with respect to this value up to second order terms. Then, one averages the obtained equation over spatial ensemble. While averaging, the first order term vanishes due to the conservation of the mean concentration. Denoting spatial mean value $\langle \Delta\nu^2(r) \rangle = 2C$, one gets equation (6). In mean field approximation, constant C should be considered as a phenomenological parameter, which characterizes microheterogeneity. At small C , the phase diagram based on (6), does not change drastically, only lowering of the critical point occurs - see fig.1. The lowering of the critical temperature (difference between tops of cupolas in fig.1) is $\Delta T = JC/8$. Shadowed area corresponds to the microheterogeneous state. Note, that this state is nonergodic: ergodic behavior leads to the phase separation according to the dashed curve.

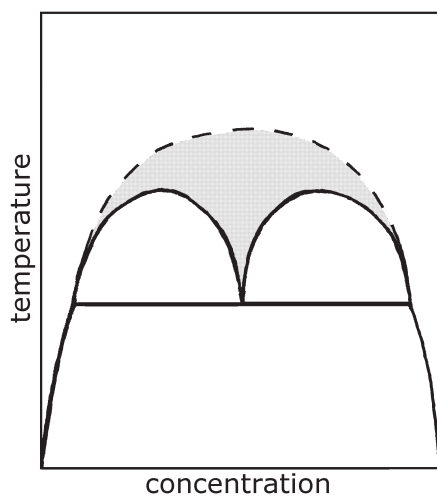


Figure 3. Bifurcation of the miscibility cupola at $C > 1/2$. Non-ergodic microheterogeneous area is shadowed.

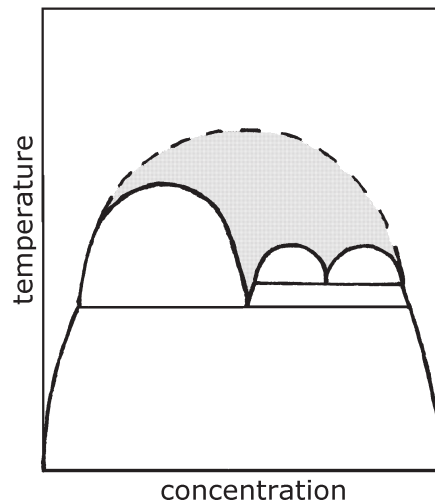


Figure 4. The small cupola corresponds to the quasi - binary system, and thus has a possibility to further splitting.

If $C > 1/2$, the shape of the phase diagram changes drastically. It splits into two cupolas, and triple point corresponding to the horizontal line in fig.3 occurs. Temperature of the tops of new cupolas T_{max} and triple point T_3 may be obtained from the analysis of (6):

$$T_3 = J \frac{E_1 - E_2}{\ln E_1 - \ln E_2} \quad (8)$$

$$T_{max} = J \left(\frac{E_{1,2}}{(1 + E_{1,2})^2} + C \frac{E_{1,2}^2 - 4E_{1,2}^3 + E_{1,2}^4}{(1 + E_{1,2})^4} \right), \quad (9)$$

where

$$E_{1,2} = \frac{5C - 1}{C + 1} \pm \sqrt{\left(\frac{5C - 1}{C + 1} \right)^2 - 1}. \quad (10)$$

Here, plus corresponds to the lower index 1, minus – to the index 2. In (9), substitution of any of two values (10) leads to the one and the same result. Above T_{max} , equation (6) has only one solution while changing ν , between T_{max} and T_3 – three stable solutions, separated by two unstable, and below T_3 – two stable, separated by one unstable. Note, that each of the two cupolas in fig.3, corresponds to the quasi – binary situation: on some intermediate space scale, the separated phases behave like two pure components, so all considerations leading to the bifurcation of the miscibility cupola may be repeated again. Thus, each of cupolas has the possibility to further splitting (fig.4)

3. Experimental status of nonergodic microheterogeneity

As an obvious experimental justification of the presented approach, we can refer to the Ga-Pb system [3], fig.2. Its behavior near the miscibility cupola in liquid state justify the theory very well. Bifurcation of the cupola and triple point are well extended also, but following considerations should be realized. In binary mixtures with limited miscibility, crystal phases may correspond to the pure components, or to several very special compositions, which have very narrow concentration intervals of existence. In fig.5, possible conjugations of diagrams in figs.1,3,4 with melting points of the pure components are presented. Fragment a) shows conjugation with the high – temperature cupola, and fragment b) – two possible variants of conjugation with low - temperature two – phase domains. Intermediate phases may be conjugated with the miscibility diagrams in the vicinity of the top of the cupola (fig.6 a), or in the vicinity of the triple point (fig.6 b).

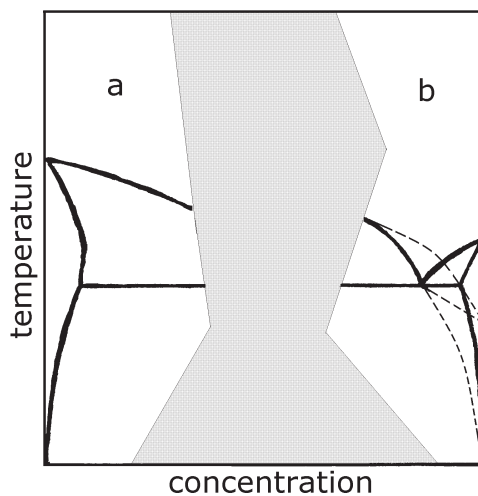


Figure 5. Possible conjugations of the miscibility curve with the melting points of pure components.

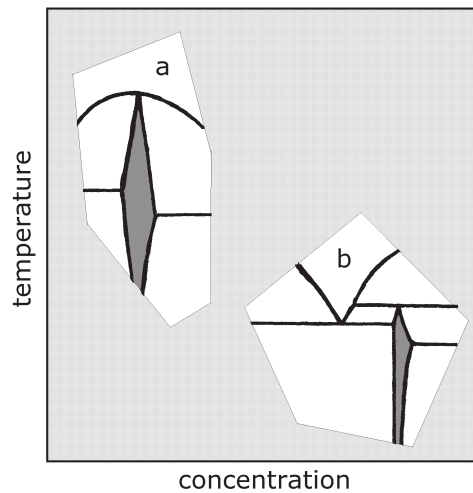


Figure 6. Possible conjugations of the miscibility curve with intermediate phase domains.

Thus, figs.1,3–6 provide possible fragments, from which phase diagrams of binary systems with limited miscibility of the components may be constructed. This provides some new look at the mentioned diagrams. In particular, our approach implies that triple point arises due to the inherent slowing down of diffusion dynamics in the liquid, and the crystallization of the products of phase separation is a supplying phenomena. Thus, slightly above eutectic points, nonergodic microheterogeneity must exist. The first example is Cu-Fe system (fig.7). Its phase diagram is constructed from elements presented in figs.1,5. The central wide two – phase domain arises from the miscibility in liquid state. This may be justified by the data on magnetic susceptibility

[5], which suggest liquid - liquid phase separation in undercooled alloy (open circles correspond to cooling, while solid - to heating). For this system, long - living microheterogeneity above the *liquidus* line was established by viscosity measurements [6]

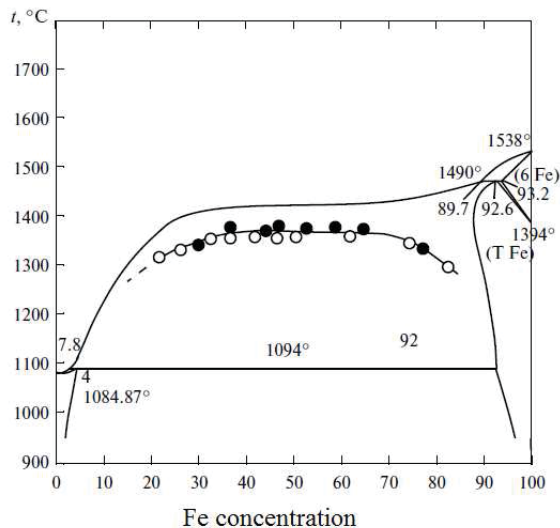


Figure 7. Cu-Fe phase diagram [4]. Undercooled cupola from magnetic susceptibility measurements is taken from [5]

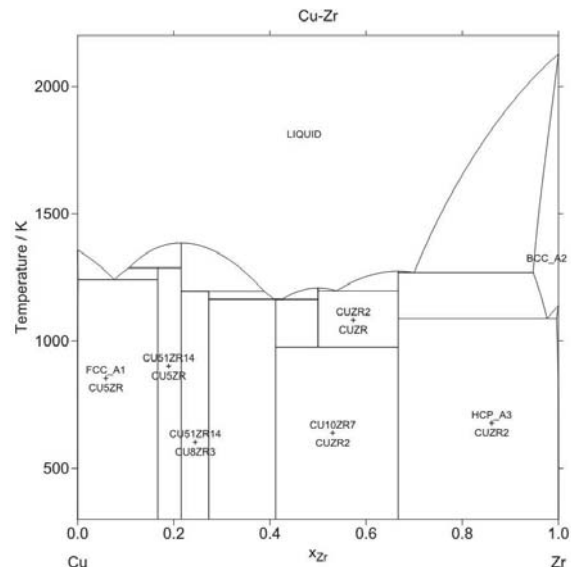


Figure 8. Cu-Zr phase diagram taken from [7]

Cu-Zr phase diagram is presented in fig.8. It may be suggested, that *Liquidus* line corresponds to four cupola splitting, afterward it was conjugated with existing crystal phases by patterns of figs.5,6. Note, that this system is strongly nonergodic, so that it can form a bulk metallic glass [8]. According to our approach, maximum of dynamic slowing down corresponds to 50% concentration, and this really the alloy with maximal glass forming ability.

Acknowledgments

The work was supported by RFBR (projects 13-03-96055, 13-03-00598, 14-02-00359) and Russian Ministry of Science and Education (Government job 2014/392 projects 2391 and 1177) One of us (L. Son) is grateful to RSCF (project 14-12-01185)

References

- [1] Son L 2014 *Journal of Non - Crystalline Solids* **401** 213
- [2] Son L D 2014 *JETP Letters* **99** 689
- [3] Filippov V and Popel P 2007 *J. Non-Cryst. Solids* **235** 3269
- [4] Turchanin M A, Agraval P G, Nikolaenko I V 2003 *J. Phase Equilibria* **24** 307
- [5] Chikova O A, Vitjunin M A, Chentsov V P, Sakun G V 2010 *Colloid Journal* **72** 2 1
- [6] Guschin V S, Shulgin D B, Baum B A, Buhler T P 1989 *Metallofizika* **11** 6 33
- [7] <http://resource.npl.co.uk/mtdata/phdiagrams/png/cuzr.png>
- [8] Inoue A, Takeuchi A 2011 *Acta Materialia* **59** 2243-2267